

AMCoR

Asahikawa Medical University Repository <http://amcor.asahikawa-med.ac.jp/>

Neuroscience (2013.4) 236:1-11.

In vivo analysis of kallikrein-related peptidase 6 (KLK6) function in oligodendrocyte development and the expression of myelin proteins.

Murakami K, Jiang YP, Tanaka T, Bando Y, Mitrovic B, Yoshida S.

Original Research Article

**In vivo analysis of kallikrein-related peptidase 6 (KLK6) function in
oligodendrocyte development and the expression of myelin proteins**

Koichi Murakami^a, Ying-Ping Jiang^{b, 1}, Tatsuhide Tanaka^a, Yoshio Bando^a, Branka

Mitrovic^{b, 2}, Shigetaka Yoshida^a.

^aDepartment of Functional Anatomy and Neuroscience, Asahikawa Medical University,

Asahikawa, Japan

^bDepartment of Immunology, Berlex Biosciences, Richmond, CA, USA

¹ Present address:

Cellerant Therapeutics, 1561 Industrial Road, San Carlos, CA 64070, USA

² Present address:

Vertex Pharmaceuticals Inc., 11010 Torreyana Road, San Diego, CA 92121, USA

Corresponding author:

Koichi Murakami, MD, PhD

Department of Functional Anatomy and Neuroscience, Asahikawa Medical University,

2-1-1-1 Midorigaoka-Higashi, Asahikawa 078-8510, Japan.

Tel: +81-166-68-2303; Fax: +81-166-68-2309; e-mail: kmura@asahikawa-med.ac.jp

This manuscript includes 63 pages and 6 figures.

Word counts: total, 7004; Abstract, 215; Introduction, 665; Experimental Procedures,
1235; Results, 1600; Discussion, 1066

Abbreviations

KLK, kallikrein-related peptidase; CNS, central nervous system; SCI, spinal cord

injury; IGF-1, insulin-like growth factor 1; GDNF, glial cell line-derived neurotrophic

factor; OPC, oligodendrocyte precursor cell; PDGF, platelet-derived growth factor; FGF,

fibroblast growth factor; EAE, experimental autoimmune encephalomyelitis; MBP,

myelin basic protein; PLP, proteolipid protein; RT-PCR, reverse

transcription-polymerase chain reaction; GAPDH, glyceraldehyde-3-phosphate

dehydrogenase; SDS, sodium dodecyl sulfate; SDS-PAGE, sodium dodecyl

sulfate-polyacrylamide gel electrophoresis; OSP, oligodendrocyte specific protein; IHC,

immunohistochemistry; PB, phosphate buffer; PBS, phosphate buffered saline; APC,

adenomatous polyposis coli; GFAP, glial fibrillary acidic protein; TUNEL,

TdT-mediated dUTP nick-end labeling; BMS, Basso Mouse Scale

Abstract

Oligodendrocytes are important for not only nerve conduction but also CNS development and neuronal survival in a variety of conditions. Kallikrein-related peptidase 6 (KLK6) is expressed in oligodendrocytes in the CNS and its expression is changed in several physiological and pathological conditions, especially following spinal cord injury (SCI) and experimental autoimmune encephalomyelitis. In this study, we investigated the functions of KLK6 in oligodendrocyte lineage cell development and the production of myelin proteins using KLK6-deficient ($KLK6^{-/-}$) mice. $KLK6^{-/-}$ mice were born without apparent defects and lived as long as wild-type (WT) mice. There was no significant difference in the numbers of oligodendrocyte precursor cells and mature oligodendrocytes in the adult naive spinal cord between WT and $KLK6^{-/-}$ mice.

However, there were fewer mature oligodendrocytes in the $KLK6^{-/-}$ spinal cord than in the WT spinal cord at postnatal day 7 (P7). Expression of myelin basic protein (MBP) and oligodendrocyte specific protein/claudin-11, major myelin proteins, was also decreased in the $KLK6^{-/-}$ spinal cord compared with the WT spinal cord at P7–21. Moreover, after SCI, the amount of MBP in the damaged spinal cords of $KLK6^{-/-}$ mice was significantly less than that in the damaged spinal cords of WT mice. These results indicate that $KLK6$ plays functional roles in oligodendrocyte development and the expression of myelin proteins.

Keywords:

Protease; spinal cord; development; myelin; spinal cord injury

Introduction

Oligodendrocytes are glial cells mainly located in the white matter of the central nervous system (CNS). The most important function of oligodendrocytes is to synthesize the myelin sheath, a lipid-rich and multilamellar structure ensheathing axons in the CNS. The myelin sheath plays a functional role in the insulation of axons and faster conduction of electrical signals, namely, saltatory conduction. The myelin sheath also functions to protect axons. For example, it protects axons against NO-induced blockade of nerve conduction (Redford et al., 1997). In addition to forming the myelin sheath, oligodendrocytes themselves are important for the maturation of axons (Colello et al., 1994, Sanchez et al., 1996). Moreover, oligodendrocytes produce several growth factors that promote the survival of neurons, such as insulin-like growth factor 1

(IGF-1), neurotrophins and glial cell line-derived neurotrophic factor (GDNF) (Du and Dreyfus, 2002).

Oligodendrocytes are derived from oligodendrocyte precursor cells (OPCs). OPCs are present not only in the developing CNS, but also in the adult brain and spinal cord.

Several factors, including platelet-derived growth factor (PDGF) (McKinnon et al., 1993, Calver et al., 1998, Tokumoto et al., 1999, Glaser et al., 2005) and fibroblast growth factor (FGF) (McKinnon et al., 1990, McKinnon et al., 1993, Calver et al., 1998), affect the proliferation and differentiation of OPCs.

Demyelination, degeneration and loss of myelin, occurs in several pathological conditions, for example, metabolic diseases (Schiffmann and van der Knaap, 2004), neurotrauma (Lu et al., 2000, Park et al., 2004), infections (Hardy et al., Berger, 2011) and demyelinating diseases (Ontaneda et al., 2012). In most cases of CNS

demyelination, oligodendrocyte death and remyelination failure occur, leading to secondary neuronal damage and degeneration. Therefore, an understanding of the mechanisms underlying oligodendrocyte development and myelination may lead to the development of new therapies for demyelinating disorders.

Kallikreins and kallikrein-related peptidases (KLKs) are serine proteases, and there are 15 family members in humans (Diamandis et al., 2000a, Diamandis et al., 2004). KLKs are known to serve a variety of physiological functions such as regulation of blood pressure, semen liquefaction and skin desquamation (Borgono et al., 2004, Sotiropoulou et al., 2009). KLKs also contribute to a wide range of pathological processes, especially tumorigenesis, angiogenesis and metastasis (Borgono and Diamandis, 2004, Borgono et al., 2004, Sotiropoulou et al., 2009). On the other hand, it is reported that KLKs play some pathogenic roles in the CNS (Diamandis et al., 2000b, Yousef et al., 2003).

In the CNS, two KLKs, KLK6/protease M/neurosin and KLK8/neurosin, are constitutively and abundantly expressed. KLK8 mRNA is constitutively expressed in the neurons of the limbic system of the adult mouse brain (Chen et al., 1995, Yoshida and Shiosaka, 1999, Shiosaka and Yoshida, 2000). We previously reported that oligodendrocytes express KLK8 in cases of spinal cord injury (SCI) (Terayama et al., 2004) and experimental autoimmune encephalomyelitis (EAE), an animal model for multiple sclerosis (Terayama et al., 2005b). Furthermore KLK8-deficient mice show milder symptoms and less oligodendrocyte loss than wild-type (WT) mice following SCI (Terayama et al., 2007) and those with EAE (Terayama et al., 2005b). These results suggest that KLK8 plays functional roles in the pathogenesis of SCI and immune-mediated demyelination.

KLK6 has been identified in human cancer cells and in the brain (Anisowicz et al.,

1996, Yamashiro et al., 1997, Yousef et al., 2003). KLK6 is constitutively expressed in oligodendrocytes in the CNS and its expression is enhanced after SCI and in EAE (Yamanaka et al., 1999, Blaber et al., 2004, Terayama et al., 2004, Terayama et al., 2005a). We previously reported that knockdown of KLK6 in cultured oligodendrocytes using RNAi suppressed the expression of the major myelin proteins myelin basic protein (MBP) and proteolipid protein (PLP) (Bando et al., 2006). These reports suggested the possibility that KLK6 plays functional roles in myelin formation in physiological and pathological conditions. However the functions of KLK6 *in vivo* have not been elucidated.

In the current study, we produced KLK6-deficient (KLK6^{-/-}) mice and investigated the function of KLK6 in oligodendrocyte lineage cell development and the expression of myelin proteins.

Experimental Procedures

Animals

pZsGreen vector (Clontech Laboratories, Mountain View, CA, USA) was used for production of the targeting vector for mouse *KLK6* gene (GeneBank ID: NC_000073) deletion. The short arm of *KLK6* gene including exon 1 and exon 2, β galactosidase gene, neomycin-resistance gene and the long arm of *KLK6* gene including exon 5 and exon 6 were inserted at the Not I site. The targeting vector was designed to replace a site containing part of exon 3 and all of exon 4 of *KLK6* gene, including the histidine of the catalytic site. The targeting vector was introduced into C57BL/6 ES cell lines and homologously recombined cells were selected using G418. The *KLK6*^{-/-} mice were

created from these mutant ES cell lines. These mutant mice and WT mice were maintained on a C57BL/6 background. Deletion of the KLK6 allele was confirmed by PCR using genomic DNA prepared from the tails and primers specific for the WT allele (sense, 5'- TTTCCAGGCTGCCCTCTACACC -3' and antisense, 5'- TTCAGGGTCCCGGAACCTATGG -3') and the mutated allele (sense, 5'- GAGGCGCGTAAGCTTCCTAGG -3' and antisense, the same primer used for the WT allele). The body weights of WT and KLK6^{-/-} mice were measured every week from 3 weeks to 10 weeks after birth (n > 10 of each genotype at all time points). At postnatal day 70, mice (n > 5 in each genotype) were killed by excess ether anesthesia and their brains were removed and weighed. All experiments were carried out in accordance with the guidelines in the U.S. National Institutes of Health Guide for the Care and Use of Laboratory Animals and as required by Asahikawa Medical University. All efforts were

made to minimize the numbers of animals used and their pain and suffering.

Reverse transcription-polymerase chain reaction (RT-PCR)

For detection of mRNA, total RNA from adult brain and spinal cord was extracted from samples using TRIzol reagent (Life Technologies, Carlsbad, CA, USA) and aliquots containing 2 µg of total RNA were used for RT with AMV-reverse transcriptase (Promega, Madison, USA), according to the manufacturer's instructions.

Aliquots from the RT reaction were then amplified by PCR. The primers used and their product sizes were as follows: KLK6 sense, 5'- CCCAGATACCATTCAGTGT -3',

antisense, 5'- CGTGGGGGAGAACTGGATGT -3' (315 bp),

glyceraldehyde-3-phosphate dehydrogenase (GAPDH) sense, 5'-

CTACATGGTCTACCTGTTCCAGT -3', antisense, 5'-
AGTTGTCATGGATGACCTTGG -3' (380 bp) and KLK8 sense, 5'-
CCCCTGCAAAAAACAGAAG -3', antisense, 5'- TGTCAGCTCCATTGCTGCT
-3' (405 bp). Thirty, 25 and 33 PCR cycles were used for KLK6, GAPDH and KLK8,
respectively. The reaction conditions were as follows: KLK6, denaturation at 94°C for
15 s, annealing at 57°C for 15 s and extension at 72°C for 45 s; GAPDH and KLK8,
denaturation at 94°C for 30 s, annealing at 60°C for 30 s and extension at 72°C for 30 s.
The reaction products were separated by electrophoresis in 1.5% agarose gels and
visualized using a transilluminator after staining with ethidium bromide. For
quantitative analysis, the LightCycler rapid thermal system (Roche Diagnostics,
Indianapolis, IN, USA) was used according to the manufacturer's protocol. The primers
used and PCR conditions were the same as above. A serially-diluted cDNA from mouse

naive spinal cord was used as a standard. The quantified data were analyzed with the LightCycler analysis software.

Western blot analysis

Mice at 1, 4, 7, 14, 21 and 70 postnatal days were killed by excess ether anesthesia (n = 4-5 of each genotype at all time points). Spinal cords were removed and homogenized in assay buffer (50 mM Tris-Cl pH 8.0, 0.1% sodium dodecyl sulfate (SDS), 0.5% sodium deoxycholate, 1% Nonidet P40 and 150 mM NaCl). The homogenates were clarified by centrifugation and the supernatant fractions were used in subsequent experiments. After determination of the protein concentration (Micro BCA Protein Assay, Thermo Scientific, Rockford, USA), 20 µg of protein was loaded onto each lane

of 15 % polyacrylamide gels for sodium dodecyl sulfate-polyacrylamide gel electrophoresis (SDS-PAGE). After electrophoresis, proteins were transferred onto an Immobilon-P membrane (Millipore, Massachusetts, USA). Immunoblotting was carried out using anti-MBP (SMI-94, mouse monoclonal, SMI-94R, Covance, New Jersey, USA, 1:5,000), anti-OSP/claudin-11 (rabbit polyclonal, ab53041, Abcam, Cambridge, UK, 1:5,000), anti-KLK6 (rabbit polyclonal, 1:500) (Terayama et al., 2005a), anti-neurofilament H (SMI-31, mouse monoclonal, NE1022, Merck Millipore, Darmstadt, Germany, 1:5,000), anti-nonphospho neurofilament (SMI-32, #17, Sternberger Monoclonals Incorporated, Lutherville, maryland, USA, 1:1,000) and anti-GAPDH (6C5, mouse monoclonal, AM4300, Life Technologies, 1:10,000) antibodies. The membranes were incubated for 1 hr at room temperature with horseradish peroxidase-conjugated secondary antibodies (GE Healthcare,

Buckinghamshire, UK, 1:5,000) and visualized using the ECL Advance Western Blotting Detection Kit (GE Healthcare) and luminescent Image Analyzer (LAS-3000, FUJIFILM, Tokyo, Japan). The intensity of each band was quantified using an image analysis program (Adobe Photoshop; Adobe Systems Inc., San Jose, CA, USA) and the amounts of the proteins were determined using a serially diluted adult spinal cord sample as a standard.

Immunohistochemistry (IHC) and Nissl staining

Mice (n = 4–5 of each genotype at all time points) were killed by excess ether anesthesia and fixed with 4% paraformaldehyde in 0.1 M phosphate buffer (PB, pH 7.4) by transcardial perfusion on postnatal days 1, 4, 7, 14, 21 and 70. Their spinal cords

were removed, postfixed overnight in the same fixative and immersed in 20% sucrose in 0.2 M PB for 2–3 days. The thoracic spinal cords were frozen in powdered dry ice and sectioned on a cryostat. The sections (18 μ m thick) were blocked with 5% bovine serum albumin in 0.1 M phosphate buffered saline (PBS) for 1 hr and incubated with primary antibodies at 4 °C overnight. The primary antibodies used were anti-KLK6 (rabbit polyclonal, 1:500) (Terayama et al., 2005a), anti-NG2 (rabbit polyclonal, AB5320, Millipore, 1:500), anti-adenomatous polyposis coli (APC) (CC1, mouse monoclonal, OP-80, Merck, Darmstadt, Germany, 1:5,000), anti-NeuN (A6, mouse monoclonal, MAB377, Millipore, 1:5,000), anti-glia fibrillary acidic protein (GFAP) (G-A-5, mouse monoclonal, G3893, Sigma, Saint Louis, Missouri, USA, 1:5,000) and anti-Iba1 (rabbit polyclonal, 019-19741, Wako, Osaka, Japan, 1:500) antibodies. After washes with 0.1 M PBS, the sections were visualized using Alexa 488-, 568- or 594-conjugated

secondary antibodies (Life Technologies, 1:500). Sections of P7 mouse spinal cord were also used for TUNEL assays, according to manufacturer's instructions (Promega).

Images were captured using a confocal microscope (FV1000-D, Olympus, Tokyo, Japan). Thionine was used for Nissl staining of spinal cord. The area of spinal cords was measured by Image J (National Institute of Health, U.S.A.).

Contusive spinal cord injury

The procedure for SCI followed the protocols of Kuhn et al. (1998). Mice (n = 5 of each genotype at all time points) were anesthetized with an intraperitoneal injection of sodium pentobarbital (40–50 mg/kg body weight). The mice were placed in a prone position and a midline incision was made in the skin. Under a dissecting microscope, a

laminectomy at the 8th thoracic (T8) level was performed and the dura mater was exposed. A 3-g weight was dropped from a height of 5 cm onto the exposed spinal cord.

After the wound was sutured, mice were allowed to survive for 12 weeks. Functional assessments were performed using the Basso Mouse Scale (BMS) (Basso et al., 2006).

Mice were evaluated in the open field for 4 min and their locomotor functions were classified into ten classes according to their capacity for hindlimb movement. “0” is the worst class with no hindlimb movement detected, and “9” is the best class with hindlimbs being moved as normal.

Statistical analysis

The significance of differences between the genotypes was assessed using the

Student's t -test.

Results

Generation of $KLK6^{-/-}$ mice

To study the function of KLK6, we created $KLK6^{-/-}$ mice on a C57BL/6 genetic background using a C57BL/6 ES cell line (Fig. 1A). $KLK6^{-/-}$ mice were born, grew and bred normally. We confirmed the deletion of the KLK6 allele by PCR using genomic DNA (data not shown). We also confirmed that expression of KLK6 mRNA and protein was lost in the adult CNS by RT-PCR, western blot analysis and immunohistochemistry (Fig. 1B-D). $KLK6^{-/-}$ mice showed no abnormal appearance on visual inspection and no motor dysfunction assessed by rotarod analysis (data not shown). We detected no difference in body weights between WT and $KLK6^{-/-}$ female mice. However, $KLK6^{-/-}$

male mice were heavier than WT male mice ($P < 0.05$ at 6 weeks after birth) (Fig. 2A).

Brain weight (Fig. 2B) and brain size (data not shown) were not different between WT

and $KLK6^{-/-}$ mice, regardless of sex. We also examined the histological structure of the

$KLK6^{-/-}$ spinal cords using Nissl staining. There was no apparent abnormality in the

spinal cords of $KLK6^{-/-}$ mice (Fig. 2C). The area of spinal cords was not different

between WT and $KLK6^{-/-}$ mice (Fig. 2D)

Reduction in the numbers of mature oligodendrocytes in the developing spinal cords

of $KLK6^{-/-}$ mice

Because $KLK6$ is expressed in oligodendrocytes of the developing and adult spinal

cord (Yamanaka et al., 1999, Terayama et al., 2004), we assumed that $KLK6$ plays

functional roles in the development and maintenance of oligodendrocytes. First, we examined the numbers of oligodendrocyte lineage cells in the spinal cords of $KLK6^{-/-}$ mice by immunohistochemistry. Oligodendrocytes are developmentally derived from oligodendrocyte precursor cells (OPCs), which differentiate into immature, premyelinating oligodendrocytes, and then finally differentiate into mature, myelinating oligodendrocytes (Nishiyama et al., 2009). We evaluated the numbers of OPCs and mature oligodendrocytes using antibodies against NG2 and adenomatous polyposis coli (APC) as cell markers for these cell types, respectively (Bhat et al., 1996, Nishiyama et al., 2009) (Fig. 3).

The number of NG2-positive OPCs in the WT spinal cord was most increased on P1 and then gradually decreased until P70 (Fig. 3I). A similar tendency was observed in the $KLK6^{-/-}$ spinal cord, and we could not detect any significant differences in the numbers

of NG2-positive OPCs between WT and $KLK6^{-/-}$ spinal cords. In contrast to the number of NG2-positive OPCs, the number of APC-positive mature oligodendrocytes in the WT spinal cord was most increased at P4 and then decreased until P21 (Fig. 3J). The $KLK6^{-/-}$ spinal cord showed a similar tendency for the numbers of APC-positive mature oligodendrocytes. However, the number of APC-positive mature oligodendrocytes in the $KLK6^{-/-}$ spinal cord was significantly lower than that in the WT spinal cord at P7 (Fig. 3C, D, J), although the numbers were not different at P14–70 (Fig. 3A, B, J). We also investigated the number of apoptotic cells in P7 spinal cord using a TUNEL assay to elucidate whether the reduction in the number of APC-positive mature oligodendrocytes in the $KLK6^{-/-}$ spinal cord was due to the increase of apoptosis of oligodendrocyte lineage cells. No TUNEL-positive apoptotic cells were detected in the ventral white matter of P7 spinal cords in mice of either genotype (data not shown),

suggesting that the reduction in the number of APC-positive mature oligodendrocytes in the P7 spinal cord of $KLK6^{-/-}$ mice was not caused by increased apoptosis of oligodendrocyte lineage cells. We also investigated the number of neurons in the ventral horn of developing spinal cords, using antibodies against NeuN as a cell marker for neurons. The number of NeuN-positive neurons in the ventral horn was most increased on P1 and then gradually decreased until P70 in both WT and $KLK6^{-/-}$ spinal cords (Fig. 3K). The number of NeuN-positive neurons in the ventral horn of $KLK6^{-/-}$ mice was significantly greater than that of WT mice at P7, although the numbers were not different at other time points examined (Fig. 3E-H, K). Small size neurons, not large size motor neurons, were prominent in the ventral horn of $KLK6^{-/-}$ spinal cord, compared with that of WT spinal cord (Fig. 3H, arrows). However, the number of NeuN-positive neurons in the whole spinal cord was not significantly different between

the genotypes (WT: 1,072/section, KLK6^{-/-}: 1,061/section). The number of GFAP-positive astrocyte and Iba1-positive microglia in the ventral white matter were not different between the genotypes at P7 (data not shown).

Reduction in the amounts of myelin proteins in the developing spinal cord of KLK6^{-/-} mice

Because the number of mature oligodendrocytes was different between WT and KLK6^{-/-} spinal cords, we next examined the expression of myelin proteins in KLK6^{-/-} spinal cords. Fig. 4 shows the expression of KLK6 and myelin proteins in developing spinal cords. KLK6 proteins could be detected in the developing spinal cords of WT mice from P4 (Fig. 4A). The expression of KLK6 protein was markedly increased at

P14 and P21 and then slightly decreased until P70 (Fig. 4B).

The expression of myelin basic protein (MBP), a major myelin protein important for myelin formation (Harauz et al., 2009), was increased postnatally until P21 and then decreased in the developing spinal cord in both genotypes (Fig. 4C). MBP expression in the $KLK6^{-/-}$ spinal cord was significantly less than that in the WT spinal cord at P7, but was not different between the genotypes from P14 to P70, as seen in the number of mature oligodendrocytes identified by the histological study (Fig. 3J). Oligodendrocyte specific protein (OSP)/claudin-11 is another major myelin protein thought to be related to tight junction formation and insulation of the myelin sheath (Devaux and Gow, 2008). Expression of OSP/claudin-11 in the spinal cord was low until P21 and drastically increased after P21 in both genotypes (Fig. 4D). OSP/claudin-11 expression in the $KLK6^{-/-}$ spinal cord was significantly lower than that in the WT spinal cord at P7 and

P21, but the expression levels were not different at P70. These results suggest that KLK6 plays a functional role in the expression of myelin proteins in developing spinal cords. Myelination process is considered to correlate with phosphorylation of neurofilament in developing spinal cords (Gotow et al., 1999), so we also investigated the amount of phosphorylated and non-phosphorylated neurofilament-H in the spinal cord at P7 by SMI-31 and SMI-32 antibodies. We could not detect significant differences in the amount of neurofilament between the genotypes (Fig. 4E).

Lower expression of MBP in the damaged spinal cords of KLK6^{-/-} mice than in WT mice

The results of the developmental study of oligodendrocytes indicated that KLK6 plays

functional roles in oligodendrocyte development and the expression of myelin proteins in immature spinal cords. In addition, the expression of KLK6 in oligodendrocytes is enhanced after SCI (Terayama et al., 2004). Therefore, we hypothesized that KLK6 may promote the expression of myelin proteins not only in developing spinal cords, but also in damaged spinal cords, which show oligodendrocyte death and myelin degeneration, and investigated the phenotype of $KLK6^{-/-}$ mice after SCI. First, we examined locomotor function after SCI, using the Basso Mouse Scale (Basso et al., 2006). In our SCI model, locomotor function started to recover from post-operative day (POD) 7 and then gradually recovered to a score of 4, indicating an ability to perform occasional plantar stepping (Fig. 5A), revealing incomplete recovery of locomotor function after SCI. BMS scores did not differ between WT and $KLK6^{-/-}$ mice after SCI, at all time points examined.

We next examined the expression of MBP in damaged spinal cords after SCI. We harvested damaged spinal cords and divided them into three parts, namely, rostral, epicenter and caudal parts (Fig. 5B), and evaluated the amount of MBP in each part (Fig. 5C-E). At POD4, the amount of MBP in the damaged spinal cords were drastically decreased in the both genotypes (Fig. 5C). The amount of MBP in the rostral part of the $KLK6^{-/-}$ spinal cord was 53% of that in the WT spinal cord (Fig. 5C-D). MBP was scarcely detected in the epicenter and caudal parts in the cords of mice of both genotypes (Fig. 5C). At POD14, The amount of MBP in the damaged spinal cord were increased (Fig. 5C). The amount of MBP in the rostral part of the $KLK6^{-/-}$ spinal cord was 54% of that in the WT spinal cord ($P < 0.01$, Fig.5 C, E). In the epicenter, the amount of MBP in the $KLK6^{-/-}$ spinal cord was 64% of that in the WT spinal cord, although this difference was not statistically significant. In contrast, there was no

difference in the level of MBP expression in the caudal part between the genotypes (Fig. 5C, E). This result shows that, in some parts of damaged $KLK6^{-/-}$ spinal cord, the expression of MBP after SCI is suppressed compared with that in WT spinal cord, suggesting functional roles for KLK6 in the expression of MBP in damaged spinal cords, as well as in developing spinal cord. To evaluate the effect on axons, we also examined the amount of neurofilament-H protein in injured spinal cord by western blot analysis, however, we could not detect significant differences in the amount of neurofilament-H in any part of injured spinal cords (data not shown).

Lower expression of KLK8 mRNA in the spinal cord of $KLK6^{-/-}$ mice than in WT mice

$KLK6^{-/-}$ mice showed no abnormal appearance and behavior in spite of loss of KLK6.

We hypothesized that other KLK family members compensate loss of KLK6, and we investigated the expression of mRNA for KLK family members. Among KLK family members, the expression of KLK8 mRNA in the KLK6^{-/-} spinal cord was lower than that in the WT spinal cord at P70 (Fig. 6).

Discussion

In this study, we show that deletion of the *KLK6* gene affects the number of oligodendrocytes and the amounts of myelin proteins in the developing spinal cord (Fig. 3, 4). In particular, the amount of MBP in damaged spinal cords was reduced in *KLK6*^{-/-} mice compared with that in WT mice (Fig. 5). These results suggest a new function for *KLK6* in promoting oligodendrocyte development and the expression of myelin proteins in the developing spinal cord and damaged spinal cords. Previous studies have reported that *KLK6* is expressed by mature oligodendrocytes in spinal cords and that its expression is enhanced in several demyelinating conditions (Blaber et al., 2004, Terayama et al., 2004, Terayama et al., 2005a). We also previously reported that knockdown of *KLK6* mRNA in cultured oligodendrocytes using RNAi suppressed the

expression of MBP and PLP (Bando et al., 2006). The results of these studies suggest a relationship between KLK6 and the expression of myelin proteins in physiological and pathological conditions.

KLK6^{-/-} mice bred normally and showed no abnormal appearance or behavior. However, KLK6^{-/-} mice were heavier than WT mice. Interestingly, this difference was detected only in male mice, not in female mice, and only at 6 weeks after birth (Fig. 2A). The reason for this phenomenon is unknown. However, changes in oligodendrocyte development and myelin protein expression in KLK6^{-/-} mice may have some effects on their growth. Further studies will be needed to elucidate the underlying mechanism.

In this study, we show that KLK6 have functional roles in oligodendrocyte development (Fig. 3). We previously reported that almost all KLK6 expressing cells are oligodendrocyte lineage cells in spinal cords (Terayama et al., 2004). In addition,

knockdown of KLK6 mRNA in oligodendrocytes using RNAi suppressed the expression of MBP and PLP in cultured conditions (Bando et al., 2006). These studies suggest that KLK6 derived from oligodendrocytes lineage cells may affect their development and the expression of myelin proteins in cell autonomous manner in vivo and in vitro.

The cleavage of extracellular proteins or their cleavage products by KLK6 may affect oligodendrocyte development and the expression of myelin proteins. KLK6 can cleave several extracellular matrix proteins and myelin proteins, including laminin, fibronectin, MBP and myelin oligodendrocyte glycoprotein (MOG) (Bernett et al., 2002, Blaber et al., 2002). These cleavage reactions and cleaved products may function in oligodendrocyte development and the expression of myelin proteins. Oligodendrocyte development is also controlled by several factors, such as PDGF, FGF, IGF, NG2 and

chemokine receptors (McKinnon et al., 1990, McKinnon et al., 1993, Calver et al., 1998, Tokumoto et al., 1999, Glaser et al., 2005, Padovani-Claudio et al., 2006, Zeger et al., 2007, Kucharova and Stallcup, 2010). KLK6 may cleave these factors or their receptors, leading to the modification of their functions related to oligodendrocyte development. Further studies are necessary to elucidate whether KLK6 does indeed cleave these molecules. The differences in the number of oligodendrocytes and the amounts of myelin proteins in developing spinal cords between KLK6^{-/-} and WT mice were temporary and disappeared by adulthood (Fig. 3, 4). Because many factors control oligodendrocyte development and the expression of myelin proteins, the involvement of KLK6 may be limited. Moreover, it is also possible that loss of KLK6 may be compensated for by other proteases in the KLK6^{-/-} spinal cord, and we found the lower expression of KLK8 mRNA in the KLK6^{-/-} spinal cord (Fig. 6). KLK8 may have

opposite functions to KLK6 in oligodendrocyte development and the expression of myelin proteins and lower expression of KLK8 may compensate loss of KLK6 function in KLK6^{-/-} spinal cords.

At P7, the number of NeuN-positive neurons in the ventral horn of KLK6^{-/-} spinal cord was greater than that of WT spinal cord (Fig. 3E-H, K). This result indicates the possibility that loss of KLK6 affect the development of not only oligodendrocyte in the white matter but also neurons in the ventral horn. Since the number of NeuN-positive neurons in the whole spinal cord was not different between genotypes, loss of KLK6 may affect the distribution of the neurons in the ventral horn, not neuronal cell death, rather than development of the neurons. However, it is unclear whether loss of KLK6 affects the development or distribution of neurons directly, or affects general development of spinal cord. Further study will be needed to elucidate this issue.

We also showed lower amounts of MBP in the damaged spinal cords of $KLK6^{-/-}$ mice than in the cords of WT mice (Fig. 5). This result suggests the involvement of KLK6 in the expression of MBP in damaged spinal cords. Although it is not possible to determine accurately that KLK6 promote remyelination of damaged spinal cords, KLK6 may have some effects on remyelination of damaged spinal cords through the expression of myelin proteins. In addition, contusive spinal cord injury induces chronic demyelination in damaged spinal cords (Totoiu et al., 2005). KLK6 may affect the expression of myelin proteins and remyelination in such chronic demyelination. Unlike KLK8, KLK6 may have protective or promoting effects on oligodendrocytes and myelin. In $KLK8^{-/-}$ mice, the functional recovery following SCI was better, and expression of MBP in the damaged spinal cord was greater than that in WT mice (Terayama et al., 2007). KLK8 may be involved in promoting oligodendrocyte death

and demyelination. A difference in the amount of MBP between WT and KLK6^{-/-} mice was observed in the rostral part, but not in the caudal part of the damaged spinal cord (Fig 5C–E). Because ascending fibers were more severely damaged in this SCI model, nerve fibers and oligodendrocytes were extensively damaged and the expression of myelin proteins was impaired in the rostral regions, manifesting as a large difference in the amount of MBP in the damaged spinal cord between the genotypes. Moreover, we could not detect any differences in locomotor function after SCI between the genotypes. This may be due to the extent of damage, which was too severe for regeneration of nerve functions.

In summary, in the present study, we showed new functions of KLK6 in the CNS. KLK6 contributes to oligodendrocyte development and the expression of myelin proteins. However, further study will be needed to elucidate the mechanisms underlying

those functions of KLK6, including the substrate of KLK6. If the mechanisms are determined, an understanding of them will lead to the development of new therapies for CNS damage and degenerating disorders, such as spinal cord injury and multiple sclerosis.

Acknowledgments

We are grateful to Mr. T. Sasaki and Mr. K. Hazawa for their technical assistance. The KLK6^{-/-} mice were designed and generated at TaconicArtemis GmbH in Cologne, Germany. This study was supported by Asahikawa Medical University (Y. Bando), grants from the Ministry of Education, Culture, Sports, Science and Technology, Japan (or the Japan Society for the Promotion of Science), Uehara Memorial Foundation (Y. Bando), Akiyama Memorial Foundation (Y. Bando) and Noastec Foundation (Y. Bando). The authors declare no financial interests.

References

Anisowicz A, Sotiropoulou G, Stenman G, Mok SC, Sager R (1996) A novel protease

homolog differentially expressed in breast and ovarian cancer. *Mol Med*

2:624-636.

Bando Y, Ito S, Nagai Y, Terayama R, Kishibe M, Jiang YP, Mitrovic B, Takahashi T,

Yoshida S (2006) Implications of protease M/neurosin in myelination during

experimental demyelination and remyelination. *Neurosci Lett* 405:175-180.

Basso DM, Fisher LC, Anderson AJ, Jakeman LB, McTigue DM, Popovich PG (2006)

Basso Mouse Scale for locomotion detects differences in recovery after spinal

cord injury in five common mouse strains. *J Neurotrauma* 23:635-659.

Berger JR (2011) The basis for modeling progressive multifocal leukoencephalopathy

pathogenesis. *Curr Opin Neurol* 24:262-267.

Bernett MJ, Blaber SI, Scarisbrick IA, Dhanarajan P, Thompson SM, Blaber M (2002)

Crystal structure and biochemical characterization of human kallikrein 6 reveals

that a trypsin-like kallikrein is expressed in the central nervous system. *J Biol*

Chem 277:24562-24570.

Bhat RV, Axt KJ, Fosnaugh JS, Smith KJ, Johnson KA, Hill DE, Kinzler KW, Baraban

JM (1996) Expression of the APC tumor suppressor protein in oligodendroglia.

Glia 17:169-174.

Blaber SI, Ciric B, Christophi GP, Bernett MJ, Blaber M, Rodriguez M, Scarisbrick IA

(2004) Targeting kallikrein 6 proteolysis attenuates CNS inflammatory disease.

Faseb J 18:920-922.

Blaber SI, Scarisbrick IA, Bernett MJ, Dhanarajan P, Seavy MA, Jin Y, Schwartz MA,

Rodriguez M, Blaber M (2002) Enzymatic properties of rat

myelencephalon-specific protease. *Biochemistry* 41:1165-1173.

Borgono CA, Diamandis EP (2004) The emerging roles of human tissue kallikreins in

cancer. *Nat Rev Cancer* 4:876-890.

Borgono CA, Michael IP, Diamandis EP (2004) Human tissue kallikreins: physiologic

roles and applications in cancer. *Mol Cancer Res* 2:257-280.

Calver AR, Hall AC, Yu WP, Walsh FS, Heath JK, Betsholtz C, Richardson WD (1998)

Oligodendrocyte population dynamics and the role of PDGF in vivo. *Neuron*

20:869-882.

Chen ZL, Yoshida S, Kato K, Momota Y, Suzuki J, Tanaka T, Ito J, Nishino H, Aimoto

S, Kiyama H, et al. (1995) Expression and activity-dependent changes of a novel

limbic-serine protease gene in the hippocampus. *J Neurosci* 15:5088-5097.

Colello RJ, Pott U, Schwab ME (1994) The role of oligodendrocytes and myelin on axon maturation in the developing rat retinofugal pathway. *J Neurosci* 14:2594-2605.

Devaux J, Gow A (2008) Tight junctions potentiate the insulative properties of small CNS myelinated axons. *J Cell Biol* 183:909-921.

Diamandis EP, Yousef GM, Clements J, Ashworth LK, Yoshida S, Egelrud T, Nelson PS, Shiosaka S, Little S, Lilja H, Stenman UH, Rittenhouse HG, Wain H (2000a) New nomenclature for the human tissue kallikrein gene family. *Clin Chem* 46:1855-1858.

Diamandis EP, Yousef GM, Olsson AY (2004) An update on human and mouse glandular kallikreins. *Clin Biochem* 37:258-260.

Diamandis EP, Yousef GM, Petraki C, Soosaipillai AR (2000b) Human kallikrein 6 as a

biomarker of alzheimer's disease. Clin Biochem 33:663-667.

Du Y, Dreyfus CF (2002) Oligodendrocytes as providers of growth factors. J Neurosci Res 68:647-654.

Glaser T, Perez-Bouza A, Klein K, Brustle O (2005) Generation of purified oligodendrocyte progenitors from embryonic stem cells. Faseb J 19:112-114.

Gotow T, Leterrier JF, Ohsawa Y, Watanabe T, Isahara K, Shibata R, Ikenaka K, Uchiyama Y (1999) Abnormal expression of neurofilament proteins in dysmyelinating axons located in the central nervous system of jimpy mutant mice. Eur J Neurosci 11:3893-3903.

Harauz G, Ladizhansky V, Boggs JM (2009) Structural polymorphism and multifunctionality of myelin basic protein. Biochemistry 48:8094-8104.

Hardy TA, Blum S, McCombe PA, Reddel SW Guillain-barre syndrome: modern

theories of etiology. *Curr Allergy Asthma Rep* 11:197-204.

Kucharova K, Stallcup WB (2010) The NG2 proteoglycan promotes oligodendrocyte

progenitor proliferation and developmental myelination. *Neuroscience*

166:185-194.

Kuhn PL, Wrathall JR (1998) A mouse model of graded contusive spinal cord injury. *J*

Neurotrauma 15:125-140.

Lu J, Ashwell KW, Waite P (2000) Advances in secondary spinal cord injury: role of

apoptosis. *Spine (Phila Pa 1976)* 25:1859-1866.

McKinnon RD, Matsui T, Dubois-Dalcq M, Aaronson SA (1990) FGF modulates the

PDGF-driven pathway of oligodendrocyte development. *Neuron* 5:603-614.

McKinnon RD, Smith C, Behar T, Smith T, Dubois-Dalcq M (1993) Distinct effects of

bFGF and PDGF on oligodendrocyte progenitor cells. *Glia* 7:245-254.

Nishiyama A, Komitova M, Suzuki R, Zhu X (2009) Polydendrocytes (NG2 cells):

multifunctional cells with lineage plasticity. *Nat Rev Neurosci* 10:9-22.

Ontaneda D, Hyland M, Cohen JA (2012) Multiple sclerosis: new insights in

pathogenesis and novel therapeutics. *Annu Rev Med* 63:389-404.

Padovani-Claudio DA, Liu L, Ransohoff RM, Miller RH (2006) Alterations in the

oligodendrocyte lineage, myelin, and white matter in adult mice lacking the

chemokine receptor CXCR2. *Glia* 54:471-483.

Park E, Velumian AA, Fehlings MG (2004) The role of excitotoxicity in secondary

mechanisms of spinal cord injury: a review with an emphasis on the implications

for white matter degeneration. *J Neurotrauma* 21:754-774.

Redford EJ, Kapoor R, Smith KJ (1997) Nitric oxide donors reversibly block axonal

conduction: demyelinated axons are especially susceptible. *Brain*

120:2149-2157.

Sanchez I, Hassinger L, Paskevich PA, Shine HD, Nixon RA (1996) Oligodendroglia

regulate the regional expansion of axon caliber and local accumulation of

neurofilaments during development independently of myelin formation. J

Neurosci 16:5095-5105.

Schiffmann R, van der Knaap MS (2004) The latest on leukodystrophies. Curr Opin

Neurol 17:187-192.

Shiosaka S, Yoshida S (2000) Synaptic microenvironments--structural plasticity,

adhesion molecules, proteases and their inhibitors. Neurosci Res 37:85-89.

Sotiropoulou G, Pampalakis G, Diamandis EP (2009) Functional roles of human

kallikrein-related peptidases. J Biol Chem 284:32989-32994. Terayama R,

Bando Y, Jiang YP, Mitrovic B, Yoshida S (2005a) Differential expression of

protease M/neurosin in oligodendrocytes and their progenitors in an animal model of multiple sclerosis. *Neurosci Lett* 382:82-87.

Terayama R, Bando Y, Murakami K, Kato K, Kishibe M, Yoshida S (2007) Neuropsin promotes oligodendrocyte death, demyelination and axonal degeneration after spinal cord injury. *Neuroscience* 148:175-187.

Terayama R, Bando Y, Takahashi T, Yoshida S (2004) Differential expression of neuropsin and protease M/neurosin in oligodendrocytes after injury to the spinal cord. *Glia* 48:91-101.

Terayama R, Bando Y, Yamada M, Yoshida S (2005b) Involvement of neuropsin in the pathogenesis of experimental autoimmune encephalomyelitis. *Glia* 52:108-118.

Tokumoto YM, Durand B, Raff MC (1999) An analysis of the early events when oligodendrocyte precursor cells are triggered to differentiate by thyroid hormone,

retinoic acid, or PDGF withdrawal. *Dev Biol* 213:327-339.

Totoiu MO, Keirstead HS (2005) Spinal cord injury is accompanied by chronic progressive demyelination, *J Comp Neurol* 486:373-383.

Yamanaka H, He X, Matsumoto K, Shiosaka S, Yoshida S (1999) Protease M/neurosin mRNA is expressed in mature oligodendrocytes. *Brain Res Mol Brain Res* 71:217-224.

Yamashiro K, Tsuruoka N, Kodama S, Tsujimoto M, Yamamura Y, Tanaka T, Nakazato H, Yamaguchi N (1997) Molecular cloning of a novel trypsin-like serine protease (neurosin) preferentially expressed in brain. *Biochim Biophys Acta* 1350:11-14.

Yoshida S, Shiosaka S (1999) Plasticity-related serine proteases in the brain (review). *Int J Mol Med* 3:405-409.

Yousef GM, Kishi T, Diamandis EP (2003) Role of kallikrein enzymes in the central nervous system. *Clin Chim Acta* 329:1-8.

Zeger M, Popken G, Zhang J, Xuan S, Lu QR, Schwab MH, Nave KA, Rowitch D,

D'Ercole AJ, Ye P (2007) Insulin-like growth factor type 1 receptor signaling in the cells of oligodendrocyte lineage is required for normal in vivo oligodendrocyte development and myelination. *Glia* 55:400-411.

Figure legends

Figure 1

Generation of $KLK6^{-/-}$ mice.

A. Gene organization and recombination of $KLK6^{-/-}$ mice. Filled boxes, exons; LacZ, β galactosidase gene; NEO, neomycin-resistance gene; Zs Green, Zoanthus sp. green fluorescent protein gene; E, EcoRI restriction site.

B. RT-PCR products from naive adult brains and spinal cords of WT and $KLK6^{-/-}$ mice.

C. Western blot analysis of the naive adult spinal cords of WT and $KLK6^{-/-}$ mice.

Glyceraldehyde-3-phosphate dehydrogenase (GAPDH) is used as an internal control.

D. Representative images of the ventral white matter of the naive spinal cords of WT and $KLK6^{-/-}$ mice stained with antibodies against KLK6 and APC at P70. Arrows

indicate APC⁺/KLK6⁺ cells. Filled boxes in the insets indicate the area of images. Scale

bar = 50 μ m.

Figure 2

Body weight and brain weight of KLK6^{-/-} mice and histological structure of the KLK6^{-/-} spinal cord.

A. Difference in body weights of WT and KLK6^{-/-} mice. The result represents the mean body weight \pm S.E.M. (**P* < 0.05, WT male vs. KLK6^{-/-} male, Student's *t*-test).

B. Brain/body weight ratios of WT and KLK6^{-/-} mice at P70. Each bar represents the mean brain/body weight ratio \pm S.E.M.

C. Nissl staining of the spinal cords of WT and KLK6^{-/-} mice at P70. Scale bar = 500 μ m.

D. The area of spinal cord of WT and $KLK6^{-/-}$ mice at P70. Each bar represents the mean area of spinal cords \pm S.E.M.

Figure 3

Immunohistochemical analysis of developing spinal cords.

A–D. Representative images of the ventral white matter of the naive spinal cord stained with antibodies against APC at P70 (A, B) and P7 (C, D) (A and C, WT; B and D, $KLK6^{-/-}$).

E–H. Representative images of the ventral horn of the naive spinal cord stained with antibodies against NeuN at P70 (E, F) and P7 (G, H) (E and G, WT; F and H, $KLK6^{-/-}$).

Arrows in (H) indicates the small size neurons.

Filled boxes in the insets indicate the area of images. Scale bar = 100 μ m.

I-K. Quantification of the numbers of NG2- (I), APC- (J), and NeuN-positive (K) cells in the ventral white matter (I, J) or ventral horn (K) of the developing spinal cord. Each bar represents the mean number \pm S.E.M. of five individual experiments. Statistical comparisons were made between WT and $KLK6^{-/-}$ mice at each time point ($*P < 0.01$, Student's *t*-test).

Figure 4

Expression analysis of myelin- and oligodendrocyte-related proteins in the developing spinal cords.

A. Western blot analysis of the expression of myelin- and oligodendrocyte-related proteins in the developing spinal cord. Note that the exposure time was adapted so that the optimal density of bands was obtained at each time point.

B-D. Quantification of the expression of KLK6 (B), MBP (C) and OSP/claudin-11 (D)

in the developing spinal cords. Each bar represents the mean expression level \pm S.E.M.

of five individual experiments. Statistical analysis were made between WT and KLK6^{-/-}

mice at each time point (**P* < 0.05, Student's *t*-test). The intensity of each band was

quantified and the amounts of the proteins were determined using a serially diluted adult

spinal cord sample as a standard.

E. Representative images of western blot analysis of the expression of phosphorylated

neurofilament-H (pNF-H) and non-phosphorylated neurofilament-H (non-pNF-H) in the

spinal cords at P7.

Figure 5

Analysis of locomotor function and myelin protein expression after spinal cord injury

(SCI).

A. Time course of locomotor function after SCI. The result represents the mean score of

Basso Mouse Scale (BMS) \pm S.E.M.

B. The scheme of harvested samples from damaged spinal cords.

C. Western blot analysis of MBP expression in the damaged spinal cords at POD 4 and

POD 14. Exposure time, MBP POD 4, 5 minutes; MBP POD 14, 5 seconds; GAPDH

POD 4, 1 minutes; GAPDH POD14, 20 seconds.

D, E. Quantification of the expression of MBP in the damaged spinal cords at POD 4

(D) and POD 14 (E). Each bar represents the mean expression level \pm S.E.M. of five

individual experiments. Statistical comparisons were made between WT and KLK6^{-/-}

mice at each time point (* $P < 0.05$, Student's *t*-test).

Figure 6

Analysis of the expression of KLK8 mRNA in the WT and KLK6^{-/-} spinal cord at P70

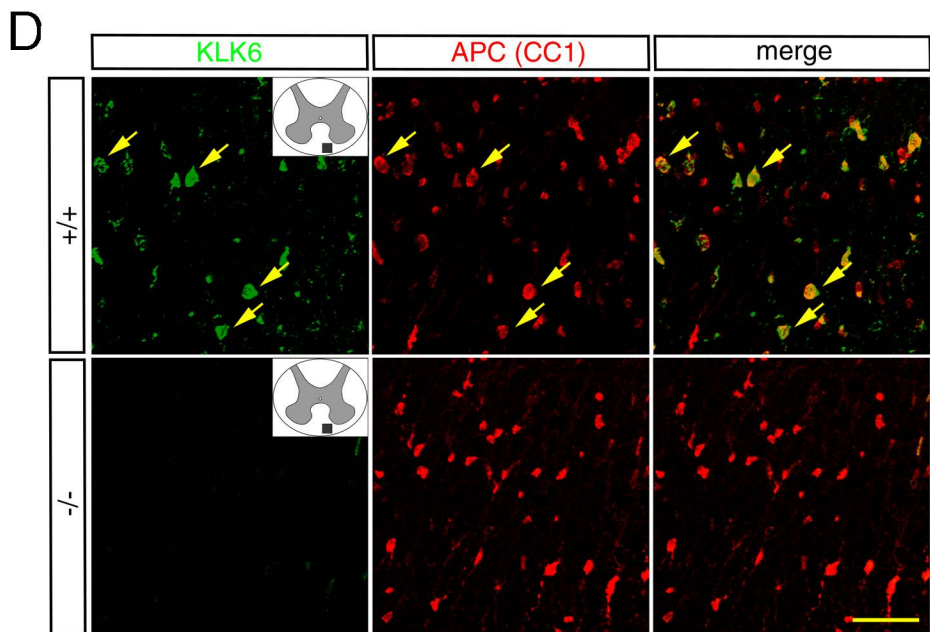
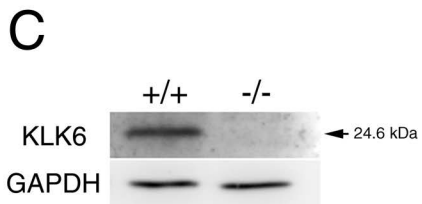
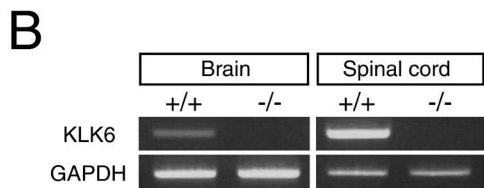
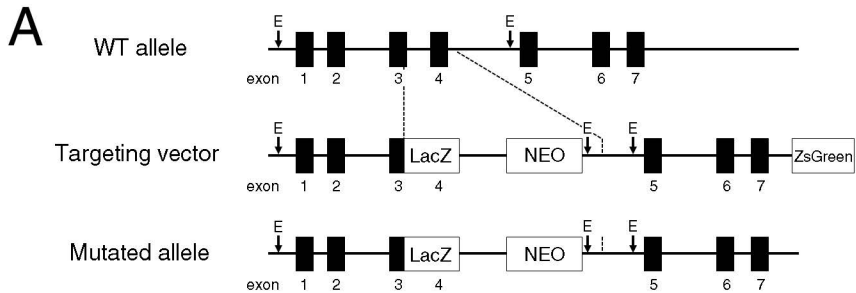
by RT-PCR.

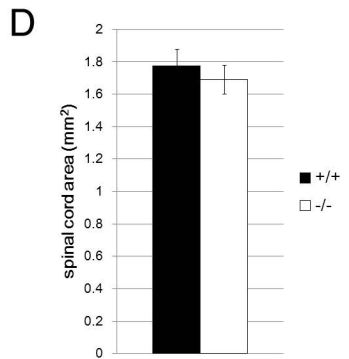
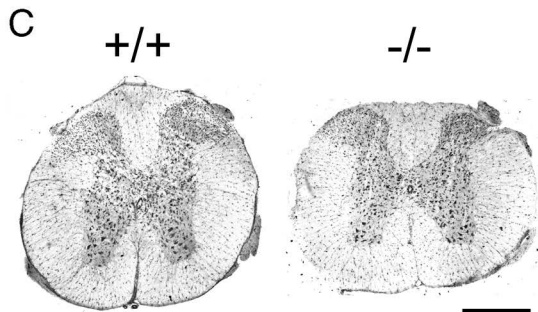
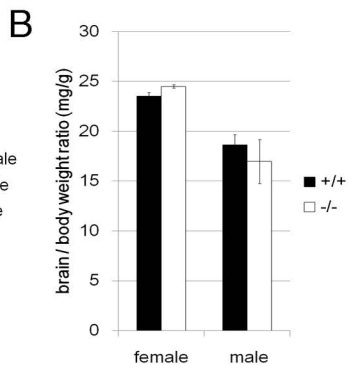
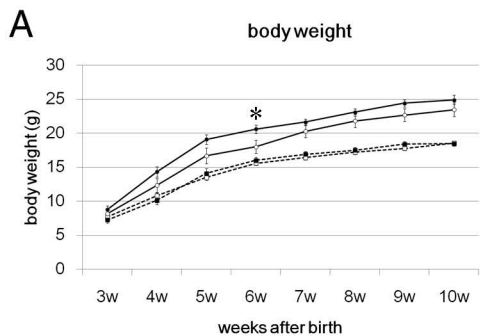
A. Representative image of RT-PCR for KLK8 and GAPDH.

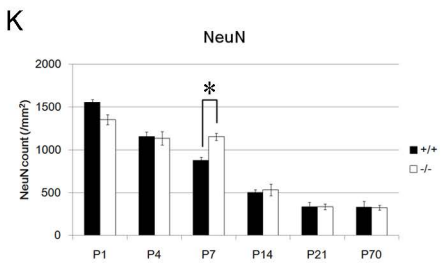
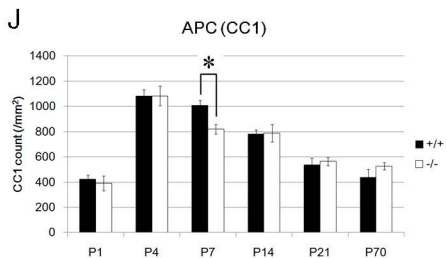
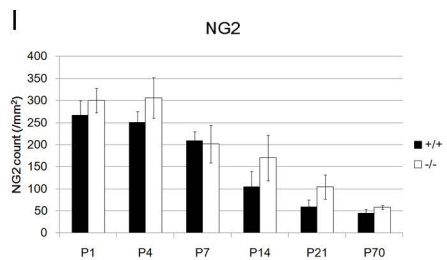
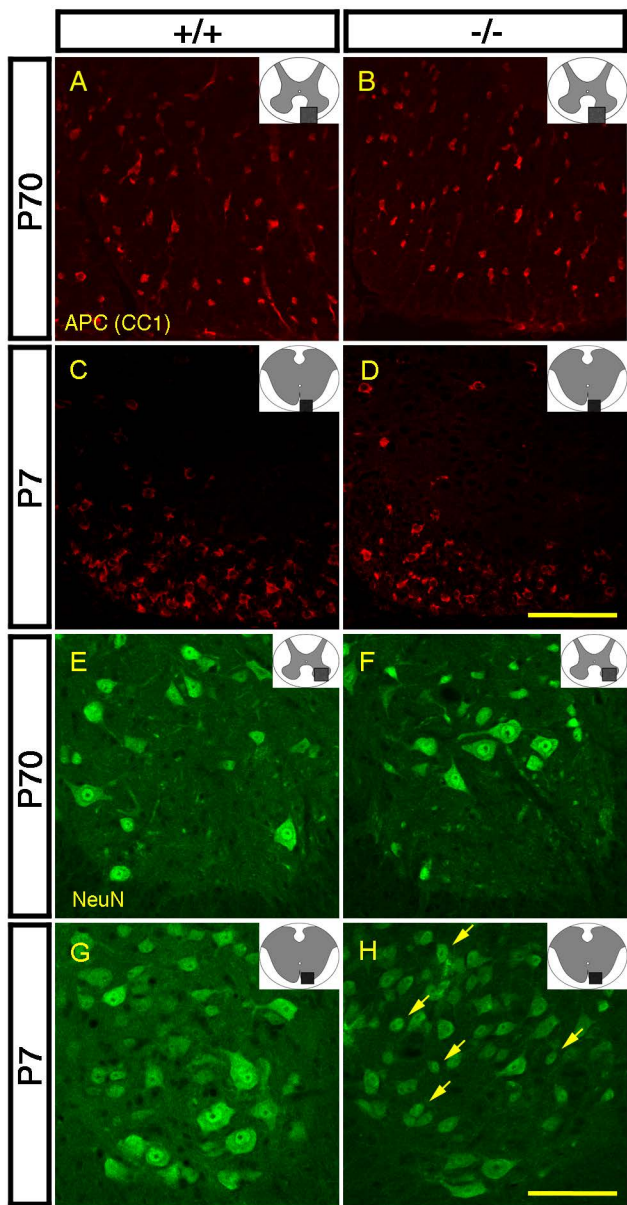
B. Quantification of the expression of KLK8 mRNA. Each bar represents the mean

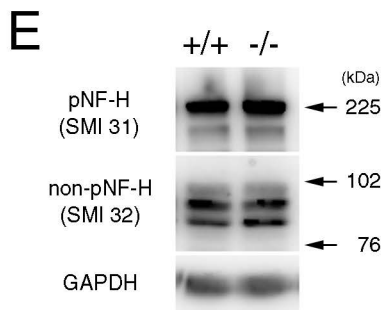
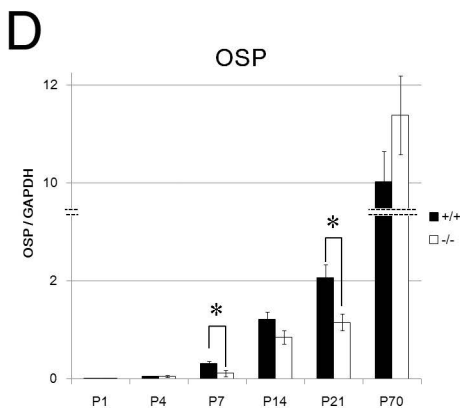
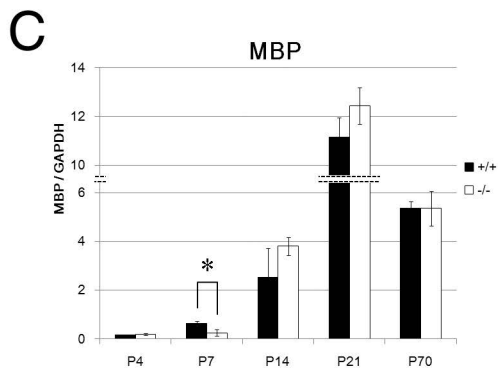
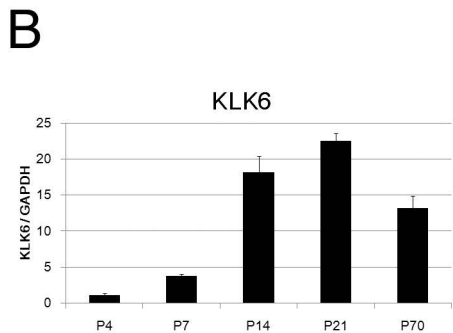
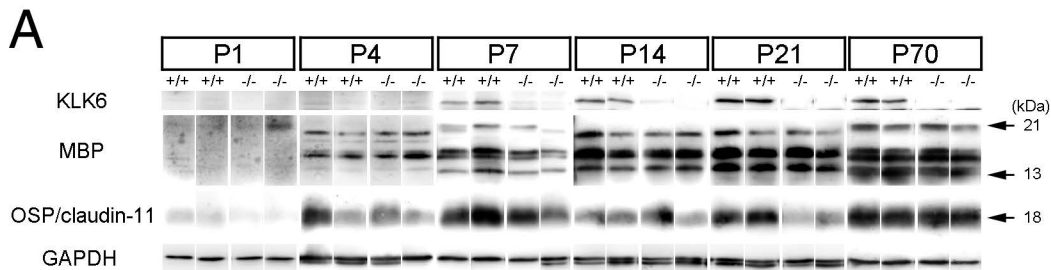
expression level \pm S.E.M. of five individual experiments. Statistical comparisons were

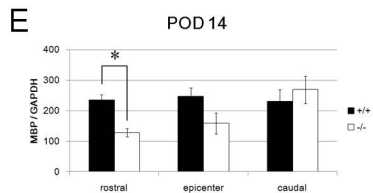
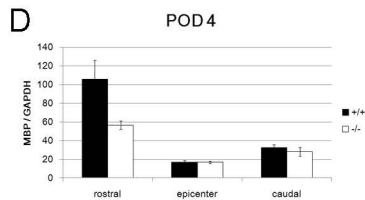
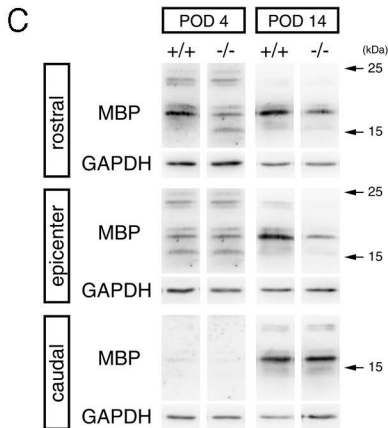
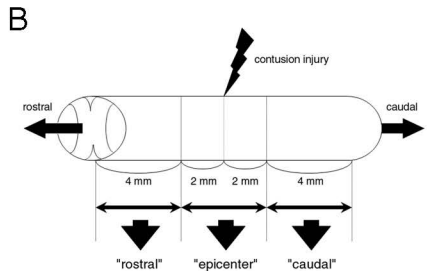
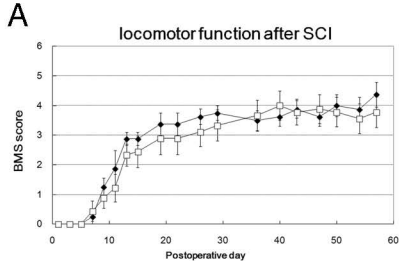
made between WT and KLK6^{-/-} mice (* $P < 0.01$, Student's *t*-test).

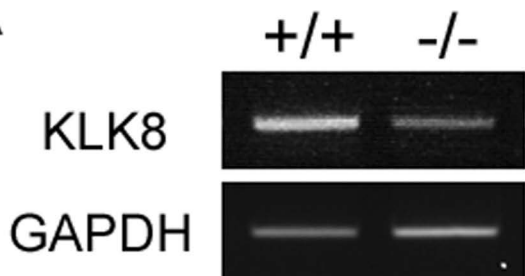










A**B**